Structuro-elasto-plasticity model for large deformation of disordered solids

Ge Zhang [⦿],[1] Hongyi Xiao [⦿],[2] Entao Yang [⦿],[3] Robert J. S. Ivancic [⦿],[4] Sean A. Ridout [⦿],[2] Robert A. Riggleman,[3] Douglas J. Durian,[2] and Andrea J. Liu [⦿][2,*]

[1]*Department of Physics, City University of Hong Kong, Hong Kong, China*
[2]*Department of Physics and Astronomy, University of Pennsylvania, Philadelphia, Pennsylvania 19104, USA*
[3]*Department of Chemical and Biomolecular Engineering, University of Pennsylvania, Philadelphia, Pennsylvania 19104, USA*
[4]*Materials Science and Engineering Division, National Institute of Standards and Technology, Gaithersburg, Maryland 20899, USA*

Elastoplastic lattice models for the response of solids to large-scale deformation typically incorporate structure only implicitly via a local yield strain that is assigned to each site. However, the local yield strain can change in response to a nearby or even distant plastic event in the system. This interplay is key to understanding phenomena such as avalanches in which one plastic event can trigger another, leading to a cascade of events, but is typically neglected in elastoplastic models. To include the interplay one could calculate the local yield strain for a given particulate system and follow its evolution, but this is expensive and requires knowledge of particle interactions that aren't necessarily pairwise additive or possible to extract from experiments. Instead, we use a structural quantity, "softness," obtained using machine learning to correlate with imminent plastic rearrangements. We show that softness correlates with local yield strain and use it to construct a "structuro-elasto-plasticity" model that reproduces particle simulation results reasonably well for several observable quantities, confirming that we capture the influence of the interplay of local structure, plasticity, and elasticity on material response.

I. INTRODUCTION

Many disordered solids exhibit ductile behavior when placed under a large mechanical load such as shear, and can be strained indefinitely without fracturing. Such systems have stress-strain curves that are monotonic except for fluctuations due to crackling noise arising from avalanches, in which one localized plastic event (particle rearrangement) triggers another and so on. The avalanches are typically described by distributions of energy and stress drops, which have power-law tails reflecting the range of avalanche sizes, from localized to extended across the entire system [1–4].

This ductile behavior is often described by a class of models known as elastoplastic (EP) models [5] that capture the interplay between elasticity and plasticity. Local regions yield (deform plastically) under sufficient elastic strain, while the plastic deformation generates elastic strain elsewhere. EP models incorporate plasticity by imposing a threshold on the amount of strain that a local region can withstand before it yields (the local yield strain). However, such models usually neglect [6], or highly simplify [7,8], the well known effects of both plasticity and elasticity on local yield strain [9]. These facilitation effects arise because local yield strain is determined by local structure. Yielding scrambles local structure, so when

a region yields, it not only changes its own local yield strain but also the local yield strains of nearby regions. Furthermore, yielding generates elastic strain, which changes more distant local yield strains.

A previous study addressed the role of local structure in ductile jammed packings of two-dimensional Hertzian bidisperse disks [10]. There, the local structure was quantified by softness [11], a machine-learned predictor of the propensity of a particle to rearrange. Softness is a weighted sum of quantities that characterize local structure and has provided useful insight into the mechanical response of disordered solids, including the size of particle rearrangements, origin of a universal yield strain [12], and precursors to shear banding [13,14].

Zhang *et al.* [10] established a simple relation describing the average change in softness due to rearrangements. Here we incorporate softness and that relation, as well as the connection between softness and local yield strain, to develop a "structuro-elasto-plastic" (StEP) model for the response of the system to applied strain. Our model connects the microscopic observations of Ref. [10] to the collective response with no tunable parameters, in contrast to EP models that typically contain parameters fitted to reproduce collective responses observed in particle simulations [5]. We obtain good agreement with simulations, validating the model.

II. PARTICLE SIMULATIONS AND STEP MODEL

The "ground truth" for this study is provided by simulation [10] of two-dimensional systems of particles with short-ranged pairwise Hertzian repulsions: $U(r) = (1 - r/\sigma)^{5/2}$, where σ is the sum of the radii of the two interacting

---

*ajliu@physics.upenn.edu

particles. We choose length and energy units such that the small particle diameter and the maximum interaction between two particles are unity. Each configuration contains $N_A = 50,000$ small particles and $N_B = 50,000$ large particles with radius ratio $r_B/r_A = 1.4$. We repeatedly apply a small strain step of $\delta\epsilon = 10^{-5}$ and minimize the potential energy to approximate quasistatic athermal shear. We studied the interplay between rearrangements, strain, and softness. Details of how we identify rearrangements are provided in Appendix A. The strain is a rank-2 tensor, which is represented by a 2-by-2 matrix $\begin{pmatrix} \epsilon_{11} & \epsilon_{12} \\ \epsilon_{21} & \epsilon_{22} \end{pmatrix}$ in 2D. The matrix has four degrees of freedom, but one is ignored because it represents rotation. The other three are the volumetric strain $k = \mathrm{Tr}(\epsilon)/2$, shear strain in the xy direction (the direction of the global shear) $\epsilon_{xy} = (\epsilon_{12} + \epsilon_{21})/2$, and shear strain in the direction orthogonal to the global shear, $\epsilon_{xx-yy} = (\epsilon_{11} - \epsilon_{22})/2$. The shear strain in these two directions together constitutes the deviatoric strain $\tilde{\epsilon}$.

We calculate local yield strain by shearing a local region of the system in a certain orientation θ [15]. Particles within a circle of radius R_c can move freely, and far-away particles that are not interacting with any particles inside R_c are ignored. The first point at which the local stress-strain curve $\sigma_\theta(\epsilon)$ decreases marks the local yield strain in this direction, $\epsilon_{Y,\theta}$. A particle's overall local yield strain, ϵ_Y, is the minimum of $\epsilon_{Y,\theta}$ over θ, since we have found that during an avalanche of our particular system, rearrangement-induced shear strain of any direction is almost equally likely to induce a future rearrangement [10]. In simulations we used $\theta = \{-85°, -75°, \ldots, 85°\}$ and $R_c = 2$. We find that increasing R_c to 3 makes the resulting local yield strain less correlated with softness, which is undesirable since our model depends on such a correlation.

The distributions of local yield strain for particles with different softness values are plotted in Fig. 1(a). We see that softer particles tend to have lower local yield strain values, as expected. For each softness, the distribution is well described by the Weibull distribution [16]:

$$P(\epsilon_Y, S) = \frac{\kappa}{\lambda}\left(\frac{\epsilon_Y}{\lambda}\right)^{\kappa-1} \exp[-(\epsilon_Y/\lambda)^\kappa], \quad (1)$$

where $\kappa(S)$ and $\lambda(S)$ characterize the distribution at each softness S. Equivalently, one can characterize the Weibull distribution in terms of κ and the mean local yield strain, $\langle\epsilon_Y\rangle = \lambda\Gamma(1 + 1/\kappa)$, where $\Gamma(x)$ is the gamma function. Fig. 1(b) shows the shape parameter $\kappa(S)$ and mean local yield strain $\langle\epsilon_Y\rangle(S)$. As we will detail later, these functions are used to draw local yield strain values at given softness values.

The StEP model is summarized in Fig. 2. The system is a square lattice of blocks. Each block is characterized by the local deviatoric strain [a 2D vector, $\tilde{\epsilon} = (\epsilon_{xy}, \epsilon_{xx-yy})$], the softness (a scalar, S), and a yield strain percentile (a scalar, which we will detail later). When the system is strained, the xy-strain is increased for each block. The amount of increment (i.e., the strain step size) is chosen to be the minimum xy-strain needed to trigger the next rearrangement, so that the model is effectively event-driven. *Beyond this, our model deviates from typical EP models in several ways.* First, the local yield strain is no longer an explicit variable with a distribution that
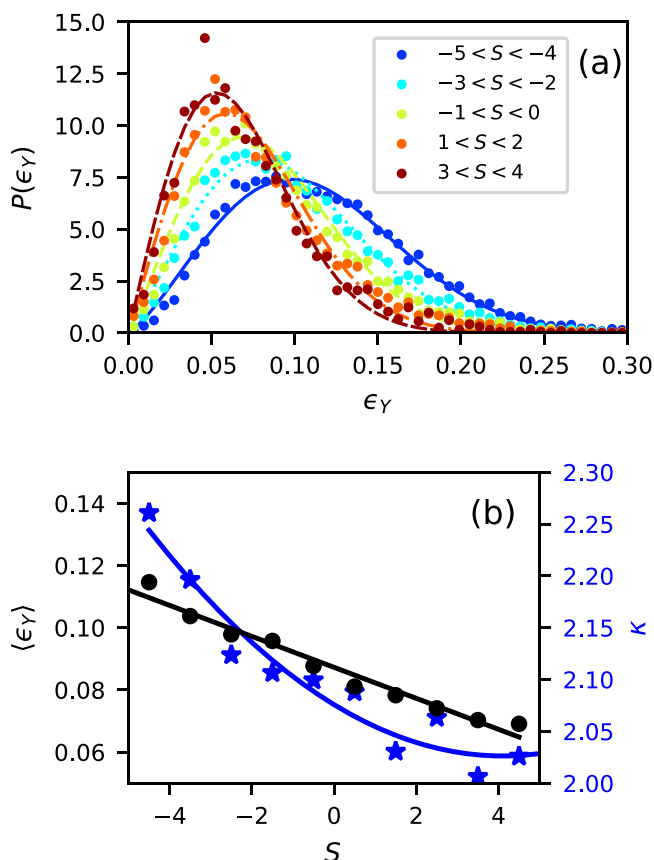
FIG. 1. (a) Probability density function (PDF) of local yield strain for particles with various softness values. Curves are Weibull distribution fits. (b) Mean local yield strain (black dots) and shape parameters (blue stars) for each softness bin. Curves are lowest-order polynomial fits, giving $\langle\epsilon_Y\rangle = 0.087 - 0.0050S$ and $\kappa = 2.08 - 0.024S + 0.0029S^2$, respectively.

is immutable and crafted by hand. Rather, it is related to softness. We initially assign to each block a softness, S_i, drawn from the softness distribution of the particle simulations [10]. It then determines the distribution of local yield strains to draw from. Upon randomly selecting $\epsilon_Y(i)$ from its distribution, we also store the percentile of the yield strain distribution
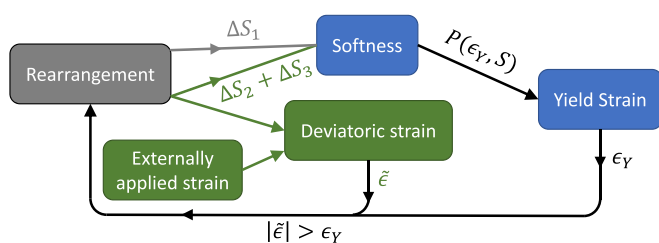
FIG. 2. Schematic of our model. A plastic strain release event at a given block changes the softness of nearby blocks, and propagates a deviatoric strain field to all other blocks. Softness determines a yield strain distribution, which in turn determines the yield strain of a block. A new rearrangement is triggered if the deviatoric strain is larger than the yield strain. Structural components are in blue, elasticity components are in green, and plasticity components are in gray; each arrow represents an equation.

corresponding to the sampled $\epsilon_Y(i)$. When a block rearranges, its yield strain percentile is redrawn and stored; otherwise the percentile is fixed, and the yield strain evolves only when S_i evolves, since changing S_i changes the distribution.

Second, we explicitly take into account both components of the deviatoric strain, not simply the xy-strain. This is because Ref. [10] found that rearrangements are triggered by both components of the deviatoric strain, not just the xy-strain, arising from other rearrangements. Once the deviatoric strain magnitude $|\tilde{\epsilon}| = \sqrt{\epsilon_{xy}^2 + \epsilon_{xx-yy}^2}$ exceeds $\epsilon_Y(i)$ and the block rearranges, it loses all of its elastic strain while the local deviatoric strain of each other block is updated through the elastic kernel function calculated using the "Fourier discretized" method [7]. However, unlike Ref. [7], we assume that the rearrangement direction aligns with the local loading direction, not with the macroscopic applied shear, so that the strain released has the same magnitude and orientation as the accumulated strain in the rearranging block. To capture this, we use four elastic kernel functions: a ϵ_{xy} to ϵ_{xy} kernel, a ϵ_{xx-yy} to ϵ_{xx-yy} kernel, and two cross-term kernels. Although the global applied strain is in the ϵ_{xy} direction, the elastic kernel functions create strain in both the ϵ_{xy} direction and the orthogonal ϵ_{xx-yy} direction, eventually making the two components' order of magnitude equal.

Third, we set the block side length equal to the small particle diameter, rather than a mesoscopic scale. This is because softness is a particle-based quantity. While softness can be coarsegrained, and it is known that tuning block size is important for obtaining good agreement with simulations in a standard EP model [8,17,18], we choose to fix it based on physical grounds instead of treating it as a parameter that can be tuned to fit simulation data. Our system size is $L = 360$ blocks per side, consistent with the side length of the particle simulations.

One result of this choice is that we cannot assume a rearrangement, which inevitably involves more than one particle, resides in a single block. As detailed in Appendix B, we find that the initial decay of the instant-time $D_{\min}^2$ correlation function in the particle simulations is well fitted by $C(r) = \exp(-r/\xi)$, where $\xi = 1.40$ provides a measure of the rearrangement size. Our measured ξ is similar to a previous result, $\xi = 1.35$, for a thermal system of 2D binary packings [19]. To incorporate these correlations into the StEP model, we assume that when a block rearranges, other blocks within a distance $r < 10$ also release strain with probability $C(r)$. These strain releases are part of the rearrangement at $r = 0$, rather than multiple independent rearrangements.

Fourth, to facilitate comparison with the simulations, we fix the timestep in the StEP model to match the simulations. As a consequence, we cannot assume that a plastic event occurs in a single timestep. The supplemental video of Ref. [10] shows that most frames in the particle simulations contain a single site of rearrangement. As detailed in Appendix C, the distance between two time frames in the simulations corresponds to a strain release of about 0.1 per unit volume. To match this in the StEP simulation, we sequentially choose the site with the largest stress overshoot, $|\tilde{\epsilon}|^2 - \epsilon_Y^2$, and let it rearrange over a period of $t = \lceil \sqrt{\sum |\tilde{\epsilon}|^2}/0.1 \rceil$ time steps, where $\lceil x \rceil$ represents the smallest integer that is larger than x,

the sum is over the rearranging site and all neighbor sites that release strain due to $C(r)$, and $\tilde{\epsilon}$ is the strain released. The amount of strain released in each timestep is thus $\tilde{\epsilon}/t$. Other sites with a stress overshoot continue to accumulate strain, but do not start rearranging until the current one finishes.

Fifth, and most important, the model allows the softness field to evolve under strain. From previous simulations [10] we know that the softness field changes whenever a rearrangement occurs, with two contributions: $\Delta S = \Delta S_1 + \Delta S_2$, corresponding to the near-field plastic and far-field elastic responses to a rearrangement at the origin, respectively. The first term describes the near-field plastic effect of a rearrangement on softness [10] and has the form $\Delta S_1 = -0.3r^{-3.1} + 0.06r^{-3.2}(\langle S \rangle - S)$. The two exponents in this equation, -3.1 and -3.2, were obtained from numerical fits. We assume their small difference is not significant and simplify this expression to

$$\Delta S_1(r) = \eta(r)(\langle S \rangle - S + c), \tag{2}$$

where $\eta(r) = 0.06r^{-3.1}$ and $c = -5$. The ΔS_2 term is proportional to the far-field volumetric strain, $k(\mathbf{r})$, due to the rearrangement. It suffices to track only the change of softness and not the volumetric strain itself, since the primary effect of this volumetric strain is to change softness. Ref. [10] showed that for the system studied here, this effect is well described by $\Delta S_2 \approx 207k(\mathbf{r})$ where $k(\mathbf{r}) = (\nu - 1)|\tilde{\epsilon}| \sin(2\theta)/(2\pi r^d)$, $\nu = 0.443$ is the Poisson's ratio, θ is the orientation of $\mathbf{r}$ relative to the orientation of the strain release, and $d = 2$ is the spatial dimension. Combining these two equations yields

$$\Delta S_2(r) = a|\tilde{\epsilon}| \sin(2\theta)r^{-d}, \tag{3}$$

where $a = -18.3$, for a strain release of $|\tilde{\epsilon}|$.

Equations (2) and (3) are empirical formulas obtained from particle simulations for the softness change in response to a rearrangement at the origin, but require three adjustments to be implemented in the StEP model. The first adjustment is to the interpretation of $\langle S \rangle$ in Eq. (2). It is unreasonable to assume that ΔS_1 is affected by the average softness value over the entire system. This problem is particularly acute in systems without time-translation symmetry. For example, if we wanted to simulate a granular pillar breaking under tensile or compressive stress, then $\langle S \rangle$ changes with time. It is hard to justify why Eq. (2), a particle-scale equation governing the evolution of softness, should contain a time-dependent parameter. To fix this problem, we replace $\langle S \rangle$ with $\langle S(r) \rangle$, the average of softness of particles at distance r to a rearranger over the most recent 1000 timesteps.

The second adjustment arises because global deviatoric strain tends to increase the average softness [12]. Our original analysis [10] did not report this effect because it was applied to avalanches (stress drops) in quasistatically sheared systems, where no strain is applied during the avalanche. We have measured the initial linear-elastic part of the stress-strain relation in our particle simulations and find that this effect indeed exists. This "loading" contribution can be summarized as the first term below:

$$\Delta S_3 = b\Delta(\tilde{\epsilon}^2) + c', \tag{4}$$
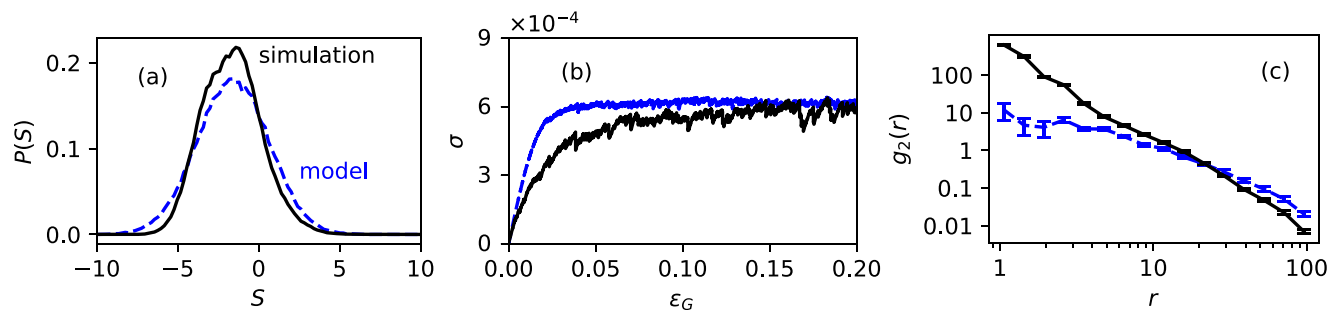
FIG. 3. Global statistics of the StEP model (blue dashed line) compared with particle simulations (black solid line), including the (a) softness distribution, (b) stress-strain curve, and (c) pair correlation function of rearrangers. The reasonable semiquantitative agreement emerges as a consequence of fixing the StEP model parameters through auxiliary measurement, not by fitting these three statistics.

where $b = 101.3$ and $\Delta(\tilde{\epsilon}^2)$ is the change of square of the elastic deviatoric strain, by symmetry. To understand the second term in Eq. (4), note that on average, Eq. (2) causes the average softness of the whole system to drop, but this is not observed in particle simulations. This suggests that there exists a term that counters the drop, which is likely spread over a sufficiently large area so that it is too small to be observed in the particle simulations in Ref. [10]. To represent this, we add a small constant softness change $c' = -c\langle\eta(r)\rangle$ to all sites, where $\langle\eta(r)\rangle$ is $\eta(r)$ numerically averaged over all sites.

Finally, Eqs. (2) and (3) describe the *average* softness change. To find the softness of a given block (i.e., particle), we have added a Gaussian-distributed random noise term, $\delta(r)$. Its magnitude is derived using a detailed balance argument detailed in Appendix D. That argument normally applies to a system in thermal equilibrium, but even for quasistatically sheared systems, an effective temperature well describes particle-level dynamics [20–23].

In summary, the softness change of a particle with softness S, at distance r from a rearrangement releasing strain ϵ is

$$\Delta S(r, S, \epsilon) = \eta(r)(\langle S(r)\rangle - S + c) + a\epsilon \sin(2\theta)r^{-\lambda}$$
$$+ b\Delta(\tilde{\epsilon}^2) + c' + \delta(r), \quad (5)$$

where all terms are separately established from particle simulations. To put the StEP model in the context of previous EP models as reviewed in Table I of Ref. [5], we include nontrivial barrier (yield strain) distributions, our plastic events have a nonzero time duration and we use elastic propagators.

III. RESULTS

The process of an avalanche in our StEP model, as well as the pattern of all rearrangements during an entire avalanche, is similar to that in particle simulations [10]. At any given time, there are only one rearrangement consisting of a few blocks releasing strain, but the total avalanche can be extended as one event triggers another, see the supplemental video [24].

We now compare quantitative results from the StEP model with the particle simulations (Fig. 3). The steady-state softness distribution is an emergent property that does not depend on the initial distribution. Here we calculate $P(S)$ by averaging over the entire run in both the StEP model and the simulations [Fig. 3(a)]. The softness distribution from the StEP model

(blue dashed curve) is in good agreement with that of the particle simulations (black solid curve).

The stress-strain curves are likewise in good agreement, as are the pair correlation function of rearrangers [Figs. 3(b) and 3(c)]. Note that while the stress-strain curve rises more sharply for the StEP model, it is monotonic with fluctuations, indicating that the system is ductile, in agreement with the simulations. Nevertheless, large stress drops in the StEP model are rarer than in particle simulations. The pair correlation function of rearrangers compares results over shorter length scales. Its agreement for $r \gtrsim 5$ demonstrates the success of our model over those length scales. In contradistinction, standard EP models are generally considered mesoscopic, with block side lengths larger than five times particle diameters [5].

We also calculate the scaling exponents of the avalanche size distributions and compare them to particle simulations for 2D overdamped Lennard-Jones systems [25], since the exponents should not be sensitive to interaction potential. For particle simulations, the rate of an energy drop of size E follows the finite-size scaling ansatz $R(E, L) = L^\beta g(E/L^\alpha)$, where L is the system length, $g(x)$ is an unknown function that scales as $x^{-\tau}$ for small x, and α and β are exponents satisfying $\beta + 2\alpha = d$ in d dimensions [25]. Defining $\gamma = \beta + \alpha\tau$, then $R(E, L) \propto L^\gamma E^{-\tau}$ for small E. Salerno and Robbins [25] found $\alpha = 0.9 \pm 0.05$, $\beta = 0.2 \pm 0.1$, $\gamma = 1.3 \pm 0.05$, and $\tau = 1.25 \pm 0.05$. As shown in Fig. 4, excellent agreement with the ansatz can be found for the StEP model with exponents $\alpha = 0.98$, $\beta = 0.04$, $\gamma = 1.30$, and $\tau = 1.29$. The ansatz holds not only for the energy-drop rate, but also for the rate of the rescaled stress drops $\Sigma = \sigma L^d$. Using Σ, we obtain scaling exponents $\alpha = 0.99$, $\beta = 0.02$, $\gamma = 1.29$, and $\tau = 1.28$. Clearly, the exponents α, γ, and τ are very similar for the StEP and particle-based calculations.

IV. DISCUSSION

In this paper, we have explicitly incorporated local structure into a standard elastoplastic (EP) framework to build a structro-elasto-plasticity (StEP) model. Elastoplastic models typically contain the effects of long-ranged elastic facilitation triggered by elastic strain arising from a rearrangement. Our model contains not only long-ranged facilitation but also short-ranged facilitation due to near-field plastic effects. The effects of such short-ranged facilitation have recently been
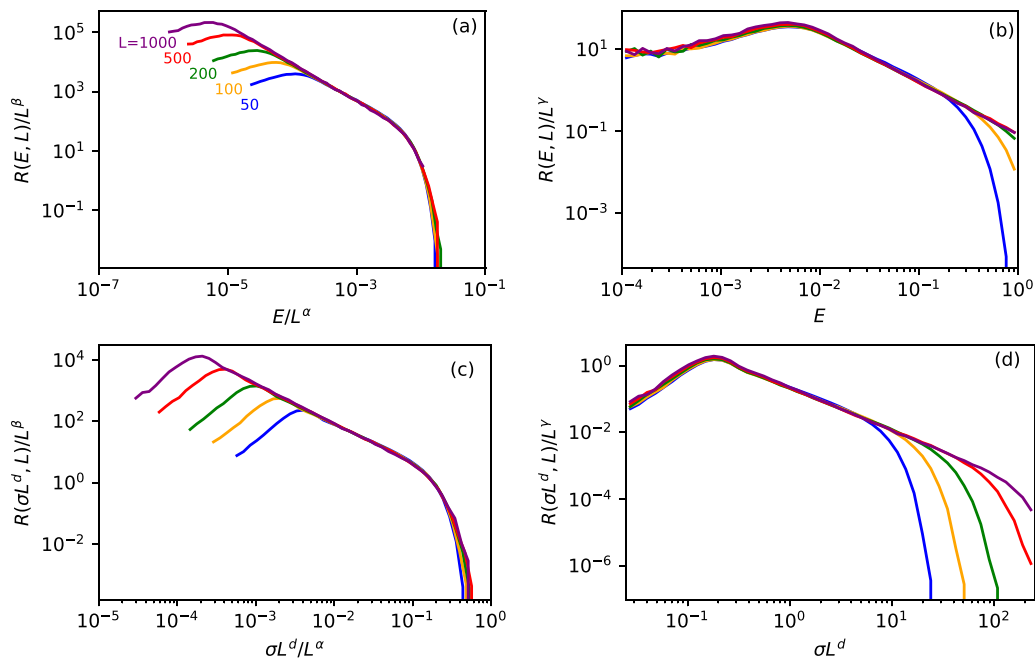
FIG. 4. Finite-size scaling collapse of energy-drop rate $R(E, L)$ for the StEP model. The curves for different system sizes align well with exponents reported in the main text. (bottom) Same as top, except for the rate of the rescaled stress drop σL^d, where $d = 2$ is the space dimension.

characterized in detail [26]. Both facilitation terms are characterized fully by parameters directly measured from numerical simulations, and our model produces results similar to those of the simulations without tuning any fitting parameters in order to match macroscopic quantities like the stress-strain curve. In contrast, standard EP models generally require empirical tuning to achieve quantitative agreement with simulations [8]. The inclusion of structural information into EP models is an important natural extension of such models, and the agreement we have achieved suggests that our model captures the key physics. Our model can be used to gain a microscopic understanding of the factors that control nonlinear mechanical response. Changes in preparation history, for example, should change only the softness distribution, while other changes will be reflected in Eq. (5), which quantifies short-ranged and elastic facilitation. The next step is to build StEP models for particle-based systems that can be tuned to varying behavior across the spectrum of ductile to brittle response.

APPENDIX A: IDENTIFYING REARRANGEMENTS IN PARTICLE SIMULATIONS

We calculate the nonaffine displacement of each particle n [27]: $D^2_{\min} = \langle (\mathbf{r}'_n - \mathbf{J}\mathbf{r}_n)^2 \rangle$, where $\langle \cdots \rangle$ indicates an average over all neighbor particles within a distance of $R_D = 2$, $\mathbf{r}_{n,}$ and

$\mathbf{r}'_n$ are the vector separations between particle n and neighbor n' during a period where the root mean squared total displacement, $\sqrt{\sum_i^N \delta \mathbf{r}_i^2}$, is 0.15. $\mathbf{J}$ is the "best-fit" local deformation gradient tensor that minimizes $D^2_{\min}$. A small/large particle "rearranges" if $D^2_{\min} > 0.0025 / D^2_{\min} > 0.0015$.

APPENDIX B: INSTANTANEOUS $D^2_{\min}$ CORRELATION FUNCTION

One component of our model is the spatial scale of a rearrangement. To measure that from the particle simulations, we calculated the $D^2_{\min}$ correlation function using the shortest possible time scale (corresponding to a strain release of 10^{-5}), shown in Fig. 5. As shown in the supplemental video of Ref.
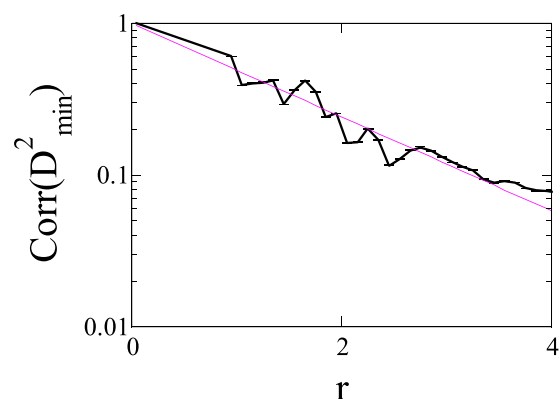
FIG. 5. The Pearson correlation function of $D^2_{\min}$ at two points with a distance of r in our particle simulation. Magenta line is the fit $\mathrm{Corr}(D^2_{\min}) = \exp(-r/1.40179)$.
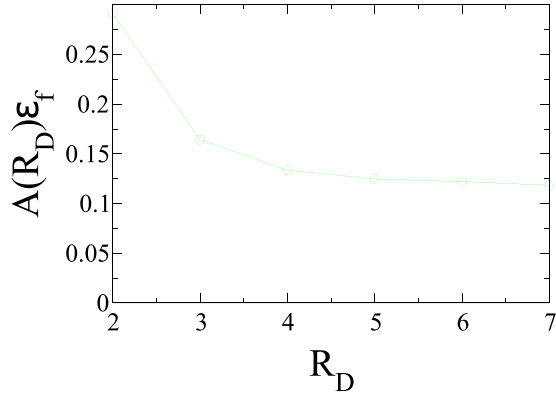
FIG. 6. The fitted deviatoric strain ε_f times the area of the fitted region $A(R_D) = \pi R_D^2$ versus the fitting radius R_D.

[10], most of these frames contain zero or one rearrangement event. Thus, this $D^2_{\min}$ correlation function measures the size of a single rearrangement rather than the spatial correlation of multiple rearrangement events.

APPENDIX C: STRAIN RELEASE PER FRAME IN PARTICLE SIMULATIONS

In particle simulations described in Ref. [10], where we studied the evolution during stress drops, we recorded a frame when the sum of particle displacement squared reached a threshold. Here we show multiple pieces of evidence that this approach leads to a deviatoric strain release of about $\epsilon = 0.1$ per unit volume per frame. The measured ϵ is used as a parameter in our StEP model, to make fair comparison of the StEP model predictions with particle simulations for the pair correlation function of rearrangers [Fig. 3(c) of the main text].

First we calculate the locally extracted deformation tensor. Within a distance of R_D from a rearranger, we perform a local fit to find the local affine deformation tensor J, and extract a deviatoric strain ε_f from J, as detailed in Ref. [10]. As shown in Fig. 6, the fitting area times ε_f approaches about 0.1 as the fitting range increases.

Second, we found earlier that the deviatoric strain field per frame caused by a rearranger is well fitted by the function $\tilde{\epsilon}(r) = 0.03 r^{-2}$ in the particle simulations, see Fig. 3 of Ref. [10]. In our StEP model, each block has a side length of 1, so for the rearranging block, the distance between its center and one of its edge is about $r = 0.5$. Thus the strain field at the edge of the block is $\tilde{\epsilon}(r = 0.5) \approx 0.1$.

Finally, we collected $N_f = 7.2 \times 10^5$ frames per unit global strain in our particle simulation. Most of these frames contain a single rearrangement. Since we have a total of $N = 10^5$ particles, and since the global strain is imposed upon each particle, the strain release per frame is roughly $N/N_f \approx 0.1$.

APPENDIX D: DETAILED BALANCE ARGUMENT FOR THE NOISE TERM

The softness change due to rearrangements in our model is captured by the sum of three terms: a restoring term, an angular term, and a noise term. We plan to use this model to study thermal systems in the future, thus we also incorporate

constraints to satisfy detailed balance. The restoring term and noise term can be correlated in the spirit of detailed balance, because rearrangements should not lead to change in average softness when the system is in equilibrium. Due to the existence of angular terms, we assume detailed balance is satisfied at each distance from the rearranger.

Our numerical measurements suggest that (1) system softness follows a Gaussian distribution, with a constant mean, μ, and variance, σ^2, during shearing ($P(S) \propto \mathcal{N}(\mu, \sigma^2)$); (2) the probability that a particle will rearrange increases exponentially with its softness ($P(R|S) \propto e^{\gamma S}$); (3) the mean softness change of a particle at a distance r from a rearranger, $\mu_R(r)$, is a linear function of the particle's current softness:

$$\mu_R(r) = \eta(r) \times (S_0(r) - S). \tag{D1}$$

This is the restoring term, where the prefactor $\eta(r)$ decays with distance r, and $S_0(r)$. We will show later that $S_0(r)$ is the average softness at r, if we assume the distribution of softness change in every step is also Gaussian:

$$P(\Delta S_R) \propto \mathcal{N}(\mu_R, \sigma_R^2). \tag{D2}$$

We start our derivation from rearranging particles. By definition, $P(R)$ is the ratio of rearranging particles over the total number of particles. Thus, for a given system at a given global strain value, the overall rearranging probability, $P(R)$, is a constant. Since detailed balance is satisfied at different distances to the rearrangers, respectively, rearranging particles ($r = 0$) themselves satisfy detailed balance:

$$P(S_1) \cdot P(R|S_1) \cdot G(S_1, S_2) = P(S_2) \cdot P(R|S_2) \cdot G(S_2, S_1), \tag{D3}$$

where $P(S)$ is particle's probability of having softness S, $P(R|S_1)$ is particle's rearranging probability when it has softness S, $G(S_1, S_2)$ is the transition probability that softness change from S_1 to S_2 after one step. By the definition above, we can write the expression of $G(S_1, S_2)$:

$$G(S_1, S_2) \propto \exp\left(-\frac{[(S_2 - S_1) - \mu_R]^2}{2\sigma_R^2}\right), \tag{D4}$$

where $\mu_R = \eta(r)(S_0(r) - S)$. Substituting it back to the detailed balance equation, we can finally see that softness of rearranging particles also follows a normal distribution:

$$P(S|R) \propto \mathcal{N}\left(S_0, \frac{\sigma_R^2}{\eta(2 - \eta)}\right). \tag{D5}$$

From Eq. (D5) above, we know that S_0 is the average softness of rearranging particles. To solve for σ_R^2, we can employ Bayes theorem:

$$P(S|R) = \frac{P(R|S) \cdot P(S)}{P(R)}. \tag{D6}$$

While $P(R)$ is a constant, $P(R|S)$ increases exponentially with softness. Thus,

$$P(S|R) \propto P(R|S) \cdot P(S) \propto \exp \gamma S \cdot \exp\left(-\frac{(S - \mu)^2}{2\sigma^2}\right)$$

$$\propto \exp\left(-\frac{(S - (\mu + \gamma\sigma^2))^2}{2\sigma^2}\right). \tag{D7}$$

Here, we get a new expression for the softness distribution of rearranging particles, $P(S|R) \propto \mathcal{N}(\mu + \gamma\sigma^2, \sigma^2)$. This leads to the first conclusion we can draw from detailed balance:

$$\frac{\sigma_R(0)^2}{\eta(0) \cdot (2 - \eta(0))} = \sigma^2. \tag{D8}$$

The standard deviation, σ_R, of softness change for rearrangers is correlated with η. For nonrearranging particles, the detailed balance equation is different:

$$P(S_1|r = r_0) \cdot G(S_1, S_2) = P(S_2|r = r_0) \cdot G(S_2, S_1), \tag{D9}$$

where $P(S_1|r = r_0)$ is the probability that we see softness S_1 at $r = r_0$. Similar as rearranging particles, we can arrive at a new expression of $P(S|r = r_0)$ by substituting all terms:

$$P(S|r_0) \propto \exp\left(-\frac{(\eta(r_0)(2 - \eta(r_0))}{2\sigma_R^2(r_0)}(S_0(r_0) - S)^2\right). \tag{D10}$$

By definition of $P(S|r_0)$, we know that $S_0(r_0)$ should be the angular average softness at $r = r_0$ (same for the the variance). This leads to the second conclus ion we can draw from detailed balance:

$$S_0(r) = \langle S(r) \rangle \tag{D11}$$

$$\frac{\sigma_R(r)^2}{\eta(r) \cdot (2 - \eta(r))} = \sigma^2. \tag{D12}$$

[1] J. P. Sethna, K. A. Dahmen, and C. R. Myers, Crackling noise, Nature (London) **410**, 242 (2001).

[2] E. K. H. Salje and K. A. Dahmen, Crackling noise in disordered mateirals, Annu. Rev. Condens. Matter Phys. **5**, 233 (2014).

[3] J. P. Sethna, M. K. Bierbaum, K. A. Dahmen, C. P. Goodrich, J. R. Greer, L. X. Hayden, J. P. Kent-Dobias, E. D. Lee, D. B. Liarte, X. Ni *et al.*, Deformation of crystals: Connections with statistical physics, Annu. Rev. Mater. Res. **47**, 217 (2017).

[4] K. A. Dahmen, J. T. Uhl, and W. J. Wright, Why the crackling deformations of single crystals, metallic glasses, rock, granular materials, and the earth's crust are so surprisingly similar, Front. Phys. **7**, 176 (2019).

[5] A. Nicolas, E. E. Ferrero, K. Martens, and J.-L. Barrat, Deformation and flow of amorphous solids: Insights from elastoplastic models, Rev. Mod. Phys. **90**, 045006 (2018).

[6] K. Martens, L. Bocquet, and J.-L. Barrat, Spontaneous formation of permanent shear bands in a mesoscopic model of flowing disordered matter, Soft Matter **8**, 4197 (2012).

[7] Z. Budrikis and S. Zapperi, Avalanche localization and crossover scaling in amorphous plasticity, Phys. Rev. E **88**, 062403 (2013).

[8] C. Liu, S. Dutta, P. Chaudhuri, and K. Martens, Elastoplastic Approach Based on Microscopic Insights for the Steady State and Transient Dynamics of Sheared Disordered Solids, Phys. Rev. Lett. **126**, 138005 (2021).

[9] A. Barbot, M. Lerbinger, A. Lemaitre, D. Vandembroucq, and S. Patinet, Rejuvenation and shear banding in model amorphous solids, Phys. Rev. E **101**, 033001 (2020).

[10] G. Zhang, S. A. Ridout, and A. J. Liu, Interplay of Rearrangements, Strain, and Local Structure during Avalanche Propagation, Phys. Rev. X **11**, 041019 (2021).

[11] S. S. Schoenholz, E. D. Cubuk, D. M. Sussman, E. Kaxiras, and A. J. Liu, A structural approach to relaxation in glassy liquids, Nat. Phys. **12**, 469 (2016).

[12] E. D. Cubuk, R. Ivancic, S. S. Schoenholz, D. Strickland, A. Basu, Z. Davidson, J. Fontaine, J. L. Hor, Y.-R. Huang, Y. Jiang *et al.*, Structure-property relationships from universal signatures of plasticity in disordered solids, Science **358**, 1033 (2017).

[13] R. J. Ivancic and R. A. Riggleman, Identifying structural signatures of shear banding in model polymer nanopillars, Soft Matter **15**, 4548 (2019).

[14] E. Yang, R. J. Ivancic, E. Y. Lin, and R. A. Riggleman, Effect of polymer–nanoparticle interaction on strain localization in polymer nanopillars, Soft Matter **16**, 8639 (2020).

[15] A. Barbot, M. Lerbinger, A. Hernandez-Garcia, R. García-García, M. L. Falk, D. Vandembroucq, and S. Patinet, Local yield stress statistics in model amorphous solids, Phys. Rev. E **97**, 033001 (2018).

[16] S. Karmakar, E. Lerner, and I. Procaccia, Statistical physics of the yielding transition in amorphous solids, Phys. Rev. E **82**, 055103(R) (2010).

[17] D. F. Castellanos, S. Roux, and S. Patinet, Insights from the quantitative calibration of an elasto-plastic model from a lennard-jones atomic glass, Comptes Rendus. Phys. **22**, 1 (2021).

[18] D. F. Castellanos, S. Roux, and S. Patinet, History dependent plasticity of glass: A mapping between atomistic and elasto-plastic models, available at http://dx.doi.org/10.2139/ssrn.4015207.

[19] R. Pastore, A. Coniglio, and M. P. Ciamarra, Spatial correlations of elementary relaxation events in glass-forming liquids, Soft Matter **11**, 7214 (2015).

[20] I. K. Ono, C. S. O'Hern, D. J. Durian, S. A. Langer, A. J. Liu, and S. R. Nagel, Effective Temperatures of a Driven System Near Jamming, Phys. Rev. Lett. **89**, 095703 (2002).

[21] L. Berthier and J.-L. Barrat, Shearing a Glassy Material: Numerical Tests of Nonequilibrium Mode-Coupling Approaches and Experimental Proposals, Phys. Rev. Lett. **89**, 095702 (2002).

[22] C. Song, P. Wang, and H. A. Makse, Experimental measurement of an effective temperature for jammed granular materials, Proc. Natl. Acad. Sci. **102**, 2299 (2005).

[23] T. K. Haxton and A. J. Liu, Activated Dynamics and Effective Temperature in a Steady State Sheared Glass, Phys. Rev. Lett. **99**, 195701 (2007).

[24] See Supplemental Material at http://link.aps.org/supplemental/10.1103/PhysRevResearch.4.043026 which is a video

depicting the course of an avalanche in our StEP model, after the global strain increases from 8.140% to 8.147%, which is just enough to trigger the avalanche.

[25] K. M. Salerno, C. E. Maloney, and M. O. Robbins, Avalanches in Strained Amorphous Solids: Does Inertia Destroy Critical Behavior? Phys. Rev. Lett. **109**, 105703 (2012).

[26] D. Richard, A. Elgailani, D. Vandembroucq, M. L. Manning, and C. E. Maloney, Mechanical excitation and marginal triggering during avalanches in sheared amorphous solids, arXiv:2202.05721.

[27] M. L. Falk and J. S. Langer, Dynamics of viscoplastic deformation in amorphous solids, Phys. Rev. E **57**, 7192 (1998).